Original article

Effect of β-cyclodextrin encapsulation on cytotoxic activity of acetylshikonin against HCT-116 and MDA-MB-231 cancer cell lines

Milena D. Vukic [a], Nenad L. Vukovic [a,*], Suzana Lj. Popovic [b], Danijela V. Todorovic [c], Predrag M. Djurdjevic [d], Sanja D. Matic [e], Marina M. Mitrovic [f], Ana M. Popovic [g], Miroslava M. Kacaniova [h,i], Dejan D. Baskic [c,j]

[a] University of Kragujevac, Faculty of Science, Department of Chemistry, R. Domanovica 12, 34000 Kragujevac, Serbia
[b] University of Kragujevac, Faculty of Medical Sciences, Centre for Molecular Medicine and Stem Cell Research, Svetozara Markovica 69, 34000 Kragujevac, Serbia
[c] University of Kragujevac, Faculty of Medical Sciences, Department of Genetics, Svetozara Markovica 69, 34000 Kragujevac, Serbia
[d] University of Kragujevac, Faculty of Medical Sciences, Department of Internal Medicine, Svetozara Markovica 69, 34000 Kragujevac, Serbia
[e] University of Kragujevac, Faculty of Medical Sciences, Doctoral Academic Studies, Svetozara Markovica 69, 34000 Kragujevac, Serbia
[f] University of Kragujevac, Faculty of Medical Sciences, Department of Biochemistry, Svetozara Markovica 69, 34000 Kragujevac, Serbia
[g] Master Academic Studies, Department of Biology and Ecology, Faculty of Sciences, University of Novi Sad, Trg Dositeja Obradovića 2, 21000 Novi Sad, Serbia
[h] Department of Fruit Sciences, Viticulture and Enology, Faculty of Horticulture and Landscape Engineering, Slovak University of Agriculture, Tr. A. Hlinku 2, 94976 Nitra, Slovakia
[i] Department of Bioenergy and Food Technology, Faculty of Biology and Agriculture, University of Rzeszow, Zelwerowicza St. 4, PL-35601 Rzeszow, Poland
[j] Public Health Institute, Nikole Pašića 1, 34000 Kragujevac, Serbia

ABSTRACT

Acetylshikonin (AcSh), as a red colored pigment found in roots of the plants from family *Boraginaceae*, showed excellent cytotoxic activity. Due to its hydrophobic nature, and thus poor bioavailability, the aim of this study was to prepare acetylshikonin/β-cyclodextrin (AcSh/β-CD) inclusion complex by using coprecipitation method, characterize obtained system by using UV/VIS, IR and ^{1}H NMR spectroscopy, and determine cytotoxic activity. Phase solubility test indicated formation of A_L-type binary system (substrate/ligand ratio was 1:1 M/M), with stability constant Ks of 306.01 M^{-1}. Formation of noncovalent bonds between inner layer of the hole of β-CD and AcSh was observed using spectroscopic methods. Notable changes in chemical shifts of two protons (−0.020 ppm) from naphthoquinone moiety (C_6-H and C_7-H), as well as protons from hydroxyl groups (−0.013 and −0.009, respectively) attached to C_5 and C_8 carbons from naphthoquinone part indicate that the molecule of AcSh enters the β-CD cavity from the aromatic side. Cytotoxic activity against HCT-116 and MDA-MB-231 cell lines was measured by MTT test and clonogenic assay. Mechanisms of action of free AcSh and inclusion complex were assessed by flow cytometry. In comparison to free AcSh, AcSh/β-CD showed stronger short-term effect on HCT-116 cells and superior long-term effect on both cell lines. Inclusion complex induced more pronounced cell cycle arrest and autophagy inhibition, and induced increase in accumulation of intracellular ROS more effectively than free AcSh. In conclusion, AcSh/β-CD binary system showed better performances regarding cytotoxic activity against tested tumor cell lines.

© 2019 The Author(s). Published by Elsevier B.V. on behalf of King Saud University. This is an open access article under the CC BY-NC-ND license (http://creativecommons.org/licenses/by-nc-nd/4.0/).

1. Introduction

As a natural naphthazarin derivative, acetylshikonin is one of the major ingredients found in red colored root extracts of the plants from family *Boraginaceae*, genera *Alkanna*, *Onosma*, *Arnebia*, *Lithospermum* and *Echium* (Papageorgiou et al., 1999; Cheng et al., 2008; Kretschmer et al., 2012; Skrzypczak et al., 2015; Vukic et al., 2017; Mirzaei et al., 2018). Acetylshikonin rich extracts have valuable usage as natural food colorants (Davis, 1988; Papageorgiou et al., 1999; Davies, 2004), while literature data have revealed that this lipophilic compound exhibits multiple pharmacological effects such as antibacterial (Papageorgiou et al., 1999; Shen et al., 2002;

Vukic et al., 2017), cytotoxic (Papageorgiou et al., 1999; Kretschmer et al., 2012; Vukic et al., 2017; Park et al., 2017), anti-inflammatory (Cheng et al., 2008; Koike, et al., 2016), antiulcer (Toker et al., 2013), antigenotoxic (Skrzypczak et al., 2015), anti-obesity (Gwon et al., 2012; Su et al., 2016) and antiparasitic (Charan Raja et al., 2016) activities.

On the other hand, lipophilic nature of naphthoquinone moiety, and thus its low water solubility, will significantly affect bioavailability and pharmaceutical efficiency of acetylshikonin. In addition, a strong influence of light and oxygen on stability of naphthazarins should be emphasized, since decomposition products showed low activities (Cheng et al., 1995, 1996a, 1996b). One approach to overcoming these problems is encapsulation with β-cyclodextrin (β-CD). From the point of the stabilization, solubilization, as well as delivery of the active ingredients, technology of encapsulation is widely used by food and pharmaceutical industries (Ozdemira et al., 2018). Previous literature data showed that β-cyclodextrin inclusion complex improved *in vivo* anti-cancer activity of curcumin (Zhang et al., 2016). Similarly, better *in vitro* cytotoxic activities were observed in cases of encapsulated norathyriol and lycorine (Han et al., 2014; Liu et al., 2017). Also, it should be noted that US Food and Drug Administration include β-cyclodextrin into GRAS (generally recognized as safe) carriers and protectants (USFDA, 2001). β-Cyclodextrin, as a member of cyclic oligosaccharides, was prepared by enzymatic degradation of starch by cyclodextrin-glycosyltransferase and contains seven (-1,4)-linked glucopyranose units (Gong et al., 2016). Together with chemical and physical stability, this molecule is characterized with a relatively hydrophobic central cavity and hydrophilic outer surface. Its low cost, as well as specific cavity size (6.0–6.5 Å diameter, 265 Å^3 volume) make this cyclic carbohydrate ideal for incorporation of guest molecules with molecular weights between 200 and 800 g/moL (Li et al., 2018). After embedding of lipophilic compounds into hydrophobic cavity of β-cyclodextrin, external microsphere of formed inclusion complex protects chemically nonaltered guest molecules from light and oxygen (Gong et al., 2016). To our knowledge, there are no studies investigating encapsulation of acetylshikonin using β-cyclodextrin and its specific cytotoxic activity.

Therefore, the objectives of the present investigation were to prepare inclusion complex of acetylshikonin with β-cyclodextrin using co-precipitation method, characterize formation of binary system by using UV/VIS, IR and ^{1}H NMR spectroscopy, and determine resulting cytotoxic activity against HCT-116 and MDA-MB-231 cancer cells.

2. Materials and methods

2.1. Materials

Pure acetylshikonin (AcSh) was isolated previously (Vukic et al., 2017). β-Cyclodextrin (β-CD), dimethyl sulfoxide-d_6 (DMSO d_6) and methanol were purchased from Sigma-Aldrich (Steinheim, Germany). Water was treated in a Milli-Q water purification system (TGI Pure Water Systems, Brea, CA, USA).

2.2. Method for preparation of inclusion complex of acetylshikonin/β-cyclodextrin

The formation of acetylshikonin/β-cyclodextrin (AcSh/β-CD) inclusion complex was done by modified method of coprecipitation (Calabro et al, 2004). Forty millilitres of deionised water and one equivalent of β-CD (343.6 mg, 3.03 × 10^{-4} mol) were added in round bottom flask. After dissolution of β-CD during continuous stirring for 1 h at room temperature, 10 mL of methanolic solution

of acetylshikonin (100 mg, 3.03 × 10^{-4} mol) was successively added. The obtained mixture was intensively stirred in a period of 3 h at 60 °C, then at room temperature for 6 h. After formation of inclusion complex, methanol was evaporated under reduced pressure by using rotary evaporator, violet precipitate of AcSh/β-CD was filtered and dried at 50 °C for 24 h.

2.3. Characterization of the complex

2.3.1. Phase solubility studies

In accordance with literature data (Higuchi and Connors, 1965), the phase solubility studies were performed in aqueous medium at room temperature and pH = 7. An excess amount of AcSh (20 mg) was added to 10 mL of deionized water with the increase of β-CD concentration (0–0.012 mol/L). Then, each of mixed solutions was stirred for 48 h at ambience temperature (25 °C) and without light. After the equilibrium had been established, all the examined solutions were filtered using a 0.45 m membrane filter to remove excess of AcSh. The absorbances of AcSh were measured by a UV/VIS spectroscopy at 520 nm. The concentrations of AcSh in tested solutions were obtained though comparing the measured values of absorbances with the standard curve of free AcSh (0.001–0.012 mol/L). This experiment was repeated three times. The apparent complexation constant (Ks) of AcSh/β-CD inclusion complex was calculated from the slope of the linear portion of the phase solubility diagrams, according to the following equation:

$$Ks = Slope/S_0(1 - Slope), \tag{1}$$

where S_0 is the solubility of AcSh in the absence of AcSh/β-CD.

2.3.2. Ultraviolet–visible (UV/VIS) spectroscopy

The UV/VIS spectra of the methanolic solutions of AcSh, AcSh/β-CD inclusion complex and β-CD were recorded in the region of 200–800 nm, by using Agilent Cary 300 UV–VIS spectrophotometer (Agilent Technologies, Palo Alto, USA).

2.3.3. Fourier transform infrared (FT-IR) spectroscopy

The FT-IR spectra of KBr pellets of AcSh, β-CD and AcSh/β-CD binary system were recorded (as KBr pills) at room temperature in a spectral region between 4000 and 450 cm^{-1} on a Thermo Scientific Nicolet 6700 FT-IR spectrometer.

2.3.4. ^{1}H NMR spectroscopy

^{1}H NMR spectra of AcSh, β-CD and AcSh/β-CD binary system were recorded on a Varian Gemini 200 spectrometer (Varian, Palo Alto, CA). Samples were dissolved in DMSO d_6 at 25 °C with tetramethylsilane (TMS) as the internal standard.

2.4. Cytotoxic activity

2.4.1. Cell cultures, drugs and chemicals

Human colorectal carcinoma (HCT-116) and human breast adenocarcinoma (MDA-MB 231) cell lines were obtained from American Type Culture Collection (ATTC, Manassas, VA, USA). Both cell lines were cultured in Dulbecco's Modified Eagle Medium (DMEM) supplemented with 10% heath-inactivated fetal bovine serum (FBS), L-glutamine (2 mM), non-essential amino acids (0.1 mM), penicillin (100 IU/mL) and streptomycin (100 g/mL) (all from Sigma, Germany) under standard culture conditions, at 37 °C in an atmosphere of 5% CO$_2$ in a humidified incubator. Cells were subcultured at 70% of confluency using combination of 0.25% trypsin and 0.53 mM EDTA and plated at 96-, 24- or 6- well microtiter plates (Thermo Scientific, New York, NY) depending on experimental design.

2.4.2. Test sample preparation

The stock solutions (50 mg/mL) of acetylshikonin (AcSh), acetylshikonin/β-cyclodextrin (AcSh/β-CD) and -cyclodextrin (β-CD) were prepared by dissolving in DMSO. The AcSh/β-CD stock was prepared according to AcSh content in complex. Afterwards, working solutions of different concentrations were prepared by diluting the stock solutions with complete medium. The final concentration of DMSO in all the experiments did not exceed 0.5% (v/v).

2.4.3. MTT assay

Cell viability was monitored by 3-(4,5-dimethylthiazol-2-yl)-2, 5-diphenyltetrazolium bromide (MTT) tetrazolium reduction assay (Mosmann, 1983), based on conversion of yellow soluble tetrazolium salt to a purple formazan by enzymes in living cells. Both cell lines were seeded in 96-well plates at density of 3×10^3 per well. After overnight incubation, the cells were treated with different concentration of AcSh, AcSh/β-CD and β-CD (1 g/mL, 3 g/mL, 10 g/mL, 30 g/mL, 100 g/mL) or supplemented media alone (control) and incubated during 24 h, 48 h and 72 h. Next, treatment solutions were removed and 100 L of freshly prepared MTT (0.5 mg/mL of MTT in un-supplemented medium) was added to each well. Following 2 h incubation period, the supernatant was discarded and DMSO (150 L) was added to solubilize the insoluble formazan purple crystals. The plates were shaken for 5 min and the absorbance was measured at 550 nm with a multiplate reader (Zenyth 3100, Anthos Labtec Instruments GmbH, Austria). All experiments were repeated at least three times in triplicates. Cell growth inhibition was calculated according to the formula: [1 − (OD Treated/OD Control (untreated))] × 100. The concentration that inhibits cellular growth by 50% compared to untreated cells (control) (IC_{50}) was calculated using Trend function in Microsoft Excel 2010.

2.4.4. Clonogenic assay

Human HTC-116 and MDA-MB-231 cells were plated into 6-well dishes with initial number of 300 cells/well and 100 cells/well, respectively. After overnight incubation, the cells were treated with acetylshikonin as well as acetylshikonin/β-cyclodextrin with five concentrations (1 g/mL, 3 g/mL, 10 g/mL, 30 g/mL, 100 g/mL). Treated cells were left to form colonies in a CO_2 incubator at 37 °C for 15 days with a regular addition of medium every fourth day. After that, the colonies were rinsed with PBS, fixed in ice-cold methanol for 15 min and stained with 10% Giemsa solution for 15 min at room temperature, photographed and counted manually, under the light microscope. The groups of more than 50 cells were scored as an individual colony. Survival fraction (SF), which represents the fraction of cell surviving a given treatment, was calculated using formula: no. of colonies formed after treatment/(no. of cells seeded × PE), where PE is defined as the ratio of the number of colonies to the number of cells seeded.

2.4.5. Flow cytometry analysis

For flow cytometric analysis experiments, HCT-116 and MDA-MB-231 cells were plated in 24-well microtiter plates at a density of 1×10^5 per well and incubated overnight for cell attachment and recovery. Subsequently, the cells were exposed to acetylshikonin and acetylshikonin/β-cyclodextrin in concentrations corresponding to their IC_{50} values or supplemented media alone (control) for 48 h at 37 °C in an atmosphere of 5% CO_2 and absolute humidity. Incubation period was terminated by harvesting cells for examination of cell cycle perturbations, expression of Bcl-2, Bax, p62 and active caspase-3. The samples were analyzed by Flow cytometer Cytomics FC500 (Beckman Coulter, USA).

2.4.6. Cell cycle analysis

Cells were seeded and treated as described in FACS analysis. After 48 h, cell monolayer was harvested, cells washed in PBS and fixed overnight with 1 mL of ice-cold ethanol at +4 °C. The fixed cells were rinsed and resuspended with PBS, incubated in presence of RNase A (500 g/mL PBS) during 30 min at room temperature and, in the final step, stained with 5 L of propidium-iodide (10 mg/mL PBS) during 15 min in dark. The DNA content was recorded by the flow cytometer and the data were analyzed using FlowJo Software (https://www.flowjo.com). Results were presented by histograms.

2.4.7. Detection and quantification of acidic vesicular organelles (AVOs) with acridine orange

Acridine orange is a cell-permeable fluorescent dye which accumulates in acid vesicles, such as lysosomes and phagolysosomes. Being protonated due to low pH, acridine orange emits bright red fluorescence in lysosomes and phagolysosomes, whereas cytoplasmic and nuclear acridine orange fluoresces bright green. Thus, it is possible to track the formation of acidic vesicular organelles (AVOs) with acridine orange staining. For detection of autophagy, at the end of treatment period, cells were collected, washed in PBS and stained with acridine orange at the final concentration of 1 g/mL for 15 min. Thereafter, cells were washed and resuspended in 300 L of PBS. Flow cytometry was used to determine the number of cells with acidic vesicular organelles. The data were analyzed using Flowing Software (http://www.flowingsoftware.com/) and expressed as percent of red/green cells.

2.4.8. Analysis of apoptosis-and autophagy-related proteins

After treatment cells were collected, washed in PBS, fixed and permeabilized using Fixation and Permeabilization Kit (eBioscience, USA). In order to verify apoptosis, the cells were incubated with primary anti-Bcl-2 (Life technologies, USA), anti-Bax (Santa Cruz Biotech Inc, USA) or anti-cleaved caspase-3 antibody (Cell signaling Technology, Danvers, USA) for 20 min at room temperature. Subsequently, the cells were washed in PBS and stained with secondary FITC-conjugated antibody (Abcam, USA) for 20 min at room temperature in the dark. After washing cells were resuspended in PBS and the samples were analyzed by flow cytometry. For autophagy detection, permeabilized cells were stained with FITC-conjugated anti-p62 monoclonal antibody (Abcam, USA). The expression of Bcl-2, Bax, and p62, presented as mean fluorescence intensity (MFI), and the percent of cells displaying cleaved caspase-3 were evaluated using Flowing Software (http://www.flowing-software.com/) and the results were presented by histograms.

2.4.9. Reactive oxygen Species assay (ROS assay)

The oxidant-sensitive dye DCFDA was used for ROS detection (DCFDA/H2DCFDA - Cellular Reactive Oxygen Species Detection Assay Kit, Abcam, USA). Briefly, cells cultured in 25 cm^2 flasks were harvested, suspended in tubes at a density of 1×10^5/mL, centrifuged, resuspended in 100 L 20 M DCFDA and incubated for 30 min at 37 °C. The cells were then treated with 100 L of corresponding IC_{50} of acetylshikonin and acetylshikonin/β-cyclodextrin inclusion complex, supplemented DMEM, or with 200 M TBHP as a positive control for 2 h, 4 h and 6 h. After incubation, 200 L of PBS was added to each tube and samples were immediately analyzed by the Flow cytometer Cytomic F500. Data from 10.000 cells per experimental condition were analyzed using Flowing Software (http://www.flowingsoftware.com/). ROS changes in treated cells were determined as percentage of control after background subtraction and the results were presented by histograms.

2.5. Statistical analysis

All experiments were carried out in three replicates and the results were presented as a mean ± standard deviation (SD). Statistical significance was determined using the Student's *t*-test. A *p* value < 0.05 was considered as significant. Statistical analysis of the data was performed using Microsoft Office Excel 2010 and SPSS commercial version 20.0 (SPSS Inc., Chicago, Illinois, USA) software. IC_{50} values (concentration that inhibited cell survival by 50%) for each cell line were calculated in Microsoft Excel 2010 using trend line.

3. Results and discussion

3.1. Phase solubility study

In order to find the stoichiometric ratio, as well as apparent stability constant (Ks) of the inclusion complex between AcSh and β-CD, phase solubility study was carried out.

As can be seen from the phase solubility diagram presented in Fig. 1, the solubility of AcSh in water linearly increased with an increased amount of β-CD, and in accordance with literature (Higuchi and Connors, 1965) can be classified as A_L-type. On the other hand, since the slope of the straight line was lower than unity, substrate/ligand ratio was 1:1 M/M. Also, apparent stability constant (Ks = 306.01 M^{-1} ± 2.11 M^{-1}) indicated that the formed inclusion complex between AcSh and β-CD was quite stable, as well as that embedded active compound would be protected against external factors with slower release from the hole of host molecule (Zyzelewicz et al., 2018).

3.2. Ultraviolet–visible (UV/VIS) spectral analysis

UV/VIS absorption spectra recorded in methanol of bioactive naphthazarin derivative, cyclic oligosaccharide and appropriate inclusion complex are presented in Fig. 2.

In accordance with literature (Zhang et al., 2016), electronic absorption spectra of β-cyclodextrin as a molecule without chromophores will not give absorptions in selected region of wavelengths (Fig. 2c). Conversely, polyunsaturated system of naphthoquinone moiety of acetylshikonin will cause existence of series of absorption bands (Fig. 2a) in ultraviolet region (at 217 nm, 231 nm and 274 nm), as well as in visible part of electromagnetic spectrum (at 488 nm, 519 nm and 560 nm). Experimental results revealed that formation of binary system, as a result of hydrophobic interaction of the coating material of the hole of β-cyclodextrin on guest molecule of acetylshikonin will
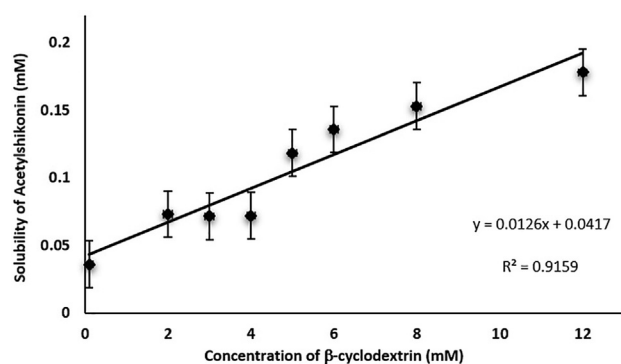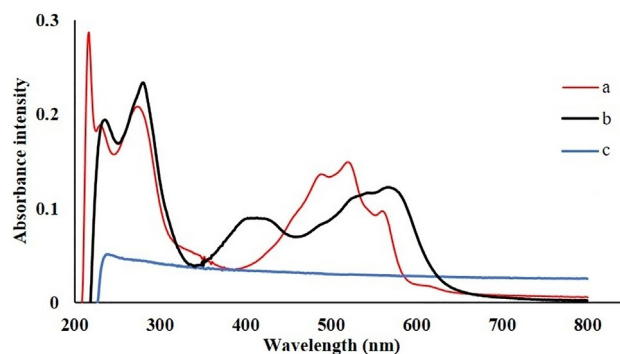

Fig. 2. UV/VIS absorption spectra of: (a) pure acetylshikonin, (b) β-cyclodextrin and (c) acetylshikonin/β-cyclodextrin inclusion complex.

reflect to perturbations of electron densities (Cheirsilp and Rakmai, 2016). Thus, for inclusion complex (Fig. 2b), two bathochromic shifted absorption maxima in ultraviolet part of spectra at 236 nm and 281 nm were observed. The visible region is characterized with one blue shifted maximum at 414 nm (in acethylshikonin at 488 nm) and two red shifted maxima at 544 nm and 566 nm (in acethylshikonin at 519 nm and 560 nm).

3.3. Fourier transform infrared (FT-IR) spectral analysis

Infrared absorption spectra of acethylshikonin, β-cyclodextrin and appropriate acethylshikonin/β-cyclodextrin inclusion complex are presented in Fig. 3.

Comparison of data of wavenumbers and intensities of absorption bands in infrared region are very important for confirmation of formation of inclusion complex (Shanmuga priya et al., 2018). Changes of wavenumbers and intensities of absorption bands of guest bioactive molecule are results of hydrophobic interactions with inner layer of host cyclodextrin cavity (modification of microenvironment and restriction of the stretching vibration). The FT-IR spectrum of AcSh (Fig. 3a) was characterized by broad band from O—H stretching vibration at 3650–3250 cm^{-1}, low intensive =C-H band at 3042 cm^{-1} from naphthoquinone moiety, series of bands from alkyl stretching vibration (at 2971 cm^{-1}, 2932 cm^{-1}, 2912 cm^{-1} and 2855 cm^{-1}), intensive ester C=O band at 1733 cm^{-1}, C=C naphthoquinone bands (at 1610 cm^{-1}, 1603 cm^{-1}, 1575 cm^{-1} and 1455 cm^{-1}) and series of bands which belong to C—O and C—O—C stretching vibrations (at 1237 cm^{-1}, 1219 cm^{-1}, 1209 cm^{-1} and 1115 cm^{-1}). These results are consistent with those previously obtained (Vukic et al., 2017). The FT-IR spectrum of β-CD (Fig. 3b) showed intensive and broad band at 3650–3140 cm^{-1} from O—H stretching vibrations, medium intensive C—H stretching vibrations at 2923 cm^{-1} and 2894 cm^{-1}, band from H-OH bending vibrations at 1647 cm^{-1}, as well as series of intensive bands which belong to C—O and C—O—C stretching vibrations (1157 cm^{-1}, 1080 cm^{-1}, 1032 cm^{-1} and 1028 cm^{-1}). Similar results had been previously observed by FT-IR analyses (Rosa et al., 2013; Amruta et al., 2018). The FT-IR spectrum of AcSh/β-CD inclusion complex (Fig. 3c) revealed intensive and broad band from O-H stretching vibrations in a region of 3670–3150 cm^{-1}, overlapped bands from C-H stretching vibrations at 2923 cm^{-1}, band which belonged to stretching vibration of ester carbonyl group at 1745 cm^{-1}, band from H-OH bending vibrations at 1614 cm^{-1}, C=C naphthoquinone bands at 1590 cm^{-1} and 1572 cm^{-1}, and series of stretching vibrations of C—O and C—O—C groups (bands at 1230 cm^{-1}, 1201 cm^{-1}, 1157 cm^{-1}, 1080 cm^{-1}, 1035 cm^{-1} and 1029 cm^{-1}, respectively). Seven glucopyranose units from the guest molecule of β-CD and its numerous O—H, C—H, C—O and C—O—C functional groups will give the most inten-

Fig. 1. The phase solubility diagram of acetylshikonin with β-cyclodextrin in distilled water at 25 °C. Values are shown as the mean ± SD of three different experiments.
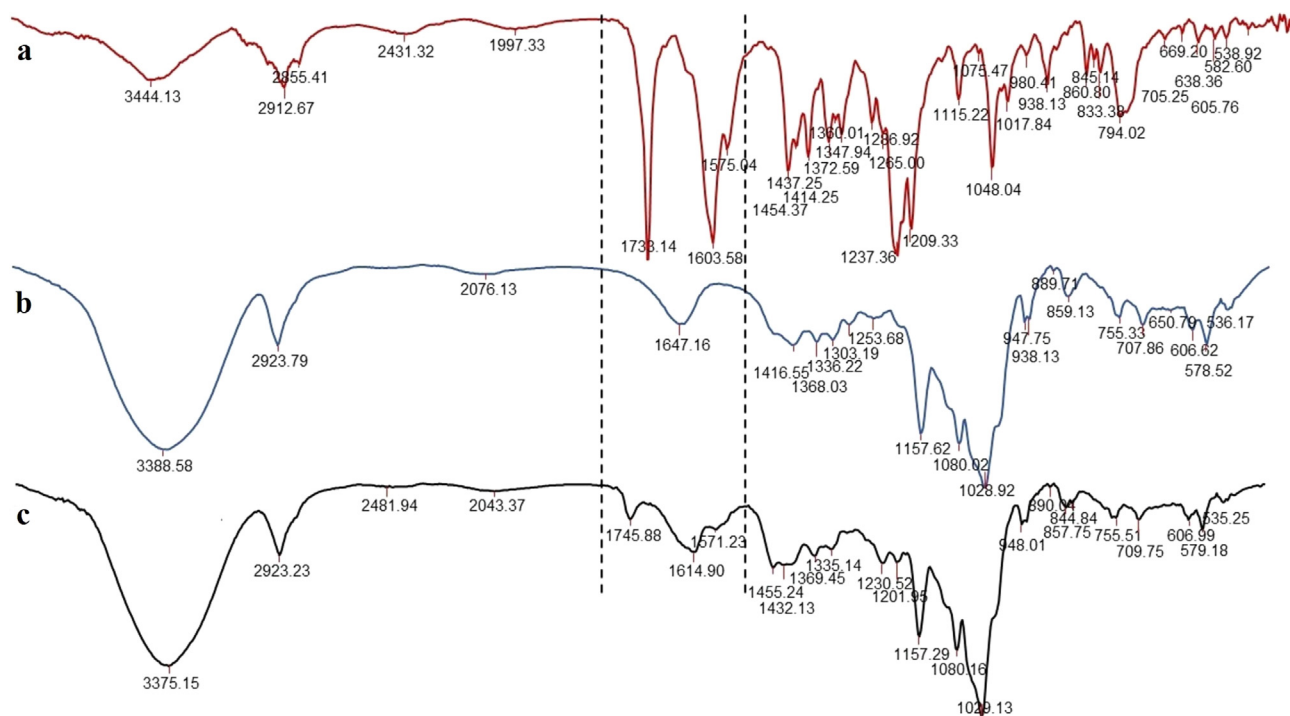
Fig. 3. FT-IR spectra of: (a) pure acetylshikonin, (b) β-cyclodextrin and (c) acetylshikonin/β-cyclodextrin inclusion complex.

sive bands in the FT-IR spectrum of formed host/guest system. Thus, inside of formed AcSh/β-CD binary system, appropriate O—H and C—H stretching vibrations from the host molecule of AcSh will be overlapped with O—H and C—H bands which belong to host molecule of β-CD. Similar situation was found for a region of C—O and C—O—C stretching vibrations. The exception was observed in a case of stretching vibrations of C—O groups from aromatic part and C—O—C ester group which give bands of low intensities shifted to lower wavenumbers (1230 cm^{-1} and 1201 cm^{-1}, respectively). Also, as a result of changing of microenvironment, C=C naphthoquinone bands absorb at lower wavenumbers (1590 cm^{-1} and 1572 cm^{-1}). Conversely, a band from stretching vibration of ester C=O group from AcSh/β-CD was observed at higher frequency (1745 cm^{-1}) then in pure AcSh. These results confirmed embedding of AcSh in AcSh/β-CD inclusion complex.

3.4. ^{1}H NMR spectral analysis

As a result of insertion of guest molecule into cavity of β-CD, variations in chemical shifts of protons will occur (Li et al., 2018). These changes are caused by the formation of noncovalent bonds, which further reflects on changed microenvironments of observed protons from guest molecule, as well as C_5-H and C_3-H protons located inside of the hole of host molecule. Thus, comparisons of ^{1}H NMR spectra of free guest molecule, host molecule of β-CD and guest/host system (together with observations of changed chemical shifts of specific spin active nucleus), will provide direct evidence of formation of inclusion complex. The ^{1}H NMR spectra of AcSh, β-CD and AcSh/β-CD binary systems are presented in Fig. 4, while the values of chemical shifts are listed in Table 1.

After embedding of AcSh, signals of C_{16}-H, C_{15}-H, $C_{2'}$-H and C_{12}-H_b protons were slightly shifted to higher fields (0.003 ppm, 0.001 ppm, 0.009 ppm and 0.002 ppm, respectively), while chemical shifts of C_{12}-Ha, C_{13}-H, C_{11}-H and C_3-H protons were observed at slightly higher frequencies (−0.003 ppm, −0.003 ppm, −0.001 ppm and −0.005 ppm, respectively). On the other hand, after complexation, two protons from naphthoquinone moiety

(C_6-H and C_7-H) were significantly shifted to lower field (−0.020 ppm) (Table 1, Fig. 4). Also, notable changes in resonances were observed for protons from hydroxyl groups attached to C_5 and C_8 carbons from naphthoquinone part (Table 1). These facts indicate that the molecule of AcSh enters the β-CD cavity from the naphthoquinone side. This mode of embedding of AcSh may be confirmed by strongly shifted signals of C_5-H and C_3-H protons (located into hydrophobic part of β-CD cavity) to lower fields (−0.037 ppm and −0.038 ppm, respectively) (Table 1, Fig. 4). Such mode of orientation of naphthoquinone moiety into the hole of β-CD will modify density of electron clouds around of C_5-H and C_3-H protons, which will result in change of shielding constants of observed protons and the appearance of their signals at higher values of chemical shifts (Fig. 5).

3.5. In vitro cytotoxic activities of acetylshikonin (AcSh) and acetylshikonin/β-cyclodextrin (AcSh/β-CD) binary system

3.5.1. Acetylshikonin/β-cyclodextrin inclusion complex exhibits cytotoxic activity against HCT-116 and MDA-MB 231 cancer cells

To explore cytotoxic effect of AcSh/β-CD inclusion complex against HCT-116 and MDA-MB-231 cancer cells and compare it to the cytotoxic effects of AcSh and β-CD, cancer cells were exposed to different concentrations (1 g/mL, 3 g/mL, 10 g/mL, 30 g/mL and 100 g/mL) of either AcSh/β-CD, free AcSh or β-CD for 24 h, 48 h and 72 h, and the percentage of cytotoxicity was determined by MTT assay (Fig. 6).

Also, IC$_{50}$ values for both cell lines were calculated (Table 2). The obtained results clearly demonstrated that the acetylshikonin/β-cyclodextrin inclusion complex displayed significant cytotoxicity against both HCT-116 and MDA-MB-231 cancer cells in a dose-dependent manner; however the time-dependent cytotoxicity of AcSh/β-CD was exhibited only in HCT-116 cells with IC$_{50}$ values of 40.8 g/mL, 11.2 g/mL and 1.2 g/mL for 24 h, 48 h and 72 h of treatments, respectively. Moreover, following 72 h treatment AcSh/β-CD exhibited significantly higher cytotoxicity toward HCT-116 cells in comparison to the cytotoxicity of free AcSh (IC$_{50}$
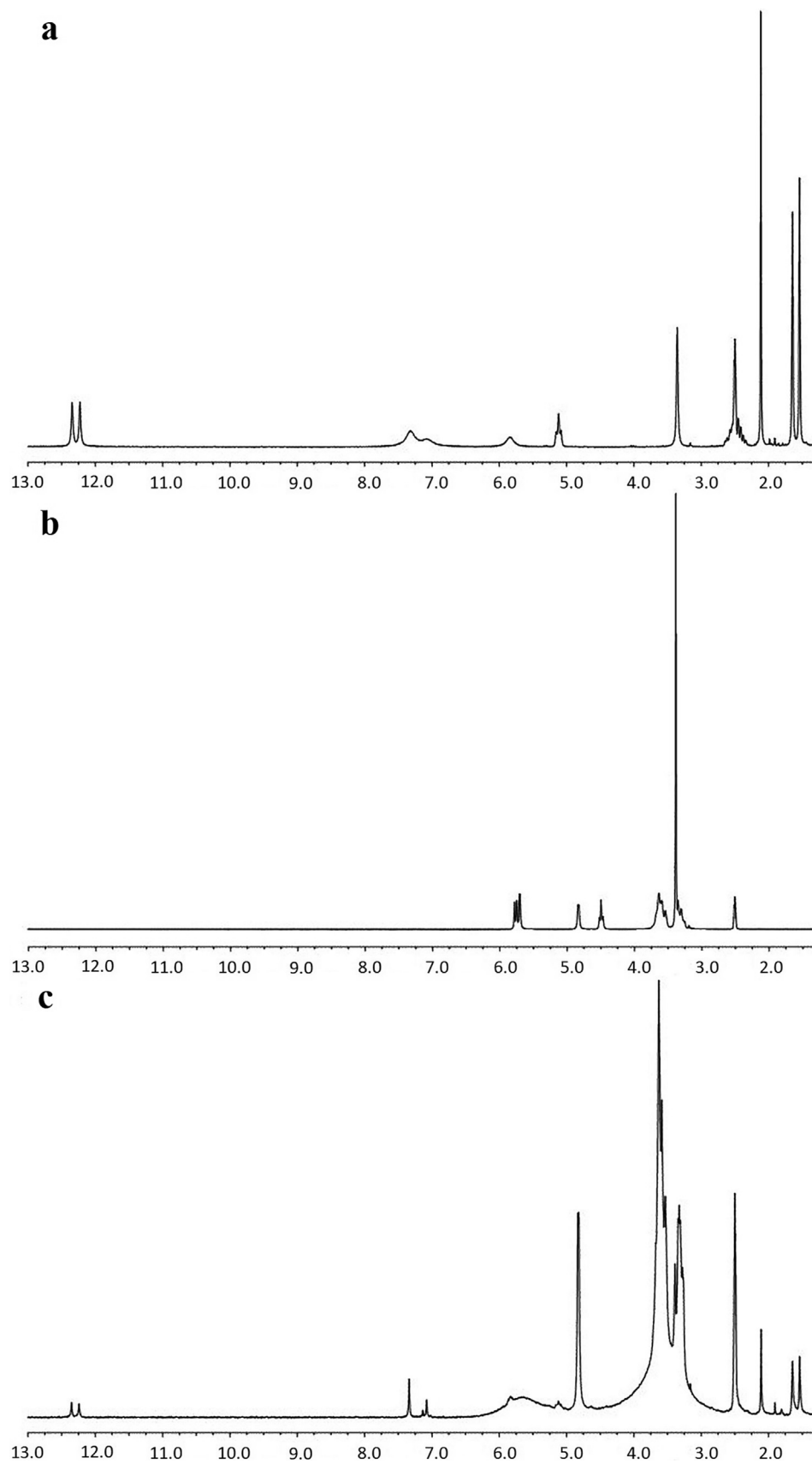
Fig. 4. ^{1}H NMR spectra of: (a) pure acetylshikonin, (b) β-cyclodextrin and (c) acetylshikonin/β-cyclodextrin binary system.

Table 1
Variation of the ^{1}H NMR chemical shifts (/ppm, DMSO d_6) of AcSh and AcSh/β-CD protons in free and in binary system.

Substance	Proton	Free (/ppm)	Binary system (/ppm)	(ppm)
AcSh	C_{16}—H	1.540	1.537	0.003
	C_{15}—H	1.645	1.644	0.001
	C_2—H	2.119	2.110	0.009
	C_{12}—Ha	2.412	2.415	−0.003
	C_{12}—Hb	2.570	2.568	0.002
	C_{13}—H	5.119	5.122	−0.003
	C_{11}—H	5.834	5.835	−0.001
	C_3—H	7.075	7.080	−0.005
	C_6—H and C_7—H	7.318	7.338	−0.020
	C_5—OH	12.229	12.242	−0.013
	C_8—OH	12.344	12.353	−0.009
β-CD	C_5—H	3.579	3.616	−0.037
	C_3—H	3.631	3.669	−0.038
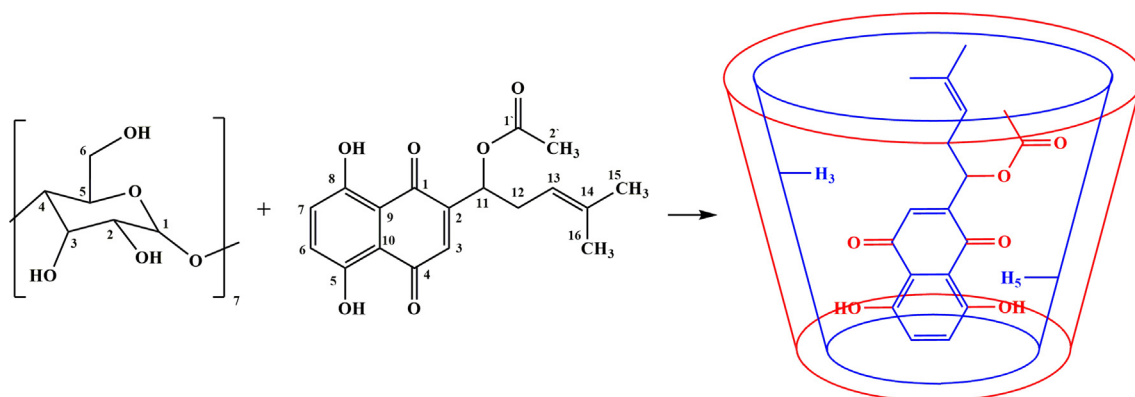
Fig 5. Possible inclusion mode of acetylshikonin into β-cyclodextrin cavity.
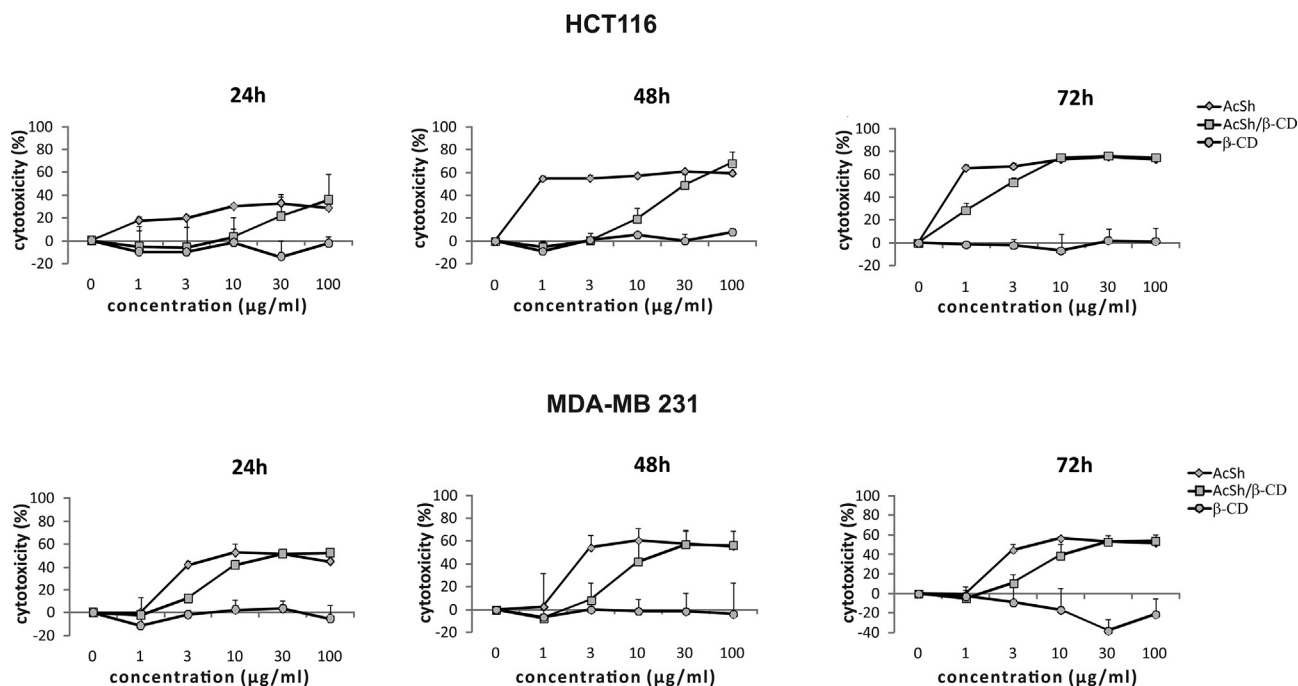
HCT116

MDA-MB 231

Fig. 6. Dose-response curves of cytotoxic effect of various concentrations of AcSh, AcSh/β-CD and β-CD against HCT-116 and MDA-MB-231 cancer cells after 24 h, 48 h and 72 h treatment, as determined by MTT assay. The obtained results are from three separate experiments presented as mean ± SD.

Table 2
IC$_{50}$ (g/mL) values of free AcSh and acetylshikonin/β-cyclodextrin (AcSh/β-CD) binary system towards HCT-116 and MDA-MB-231 cells after 24 h, 48 h and 72 h of treatment, as determined by MTT assay.

| Cell lines | [a]IC$_{50}$ (g/mL) | | | | | |
| | HCT-116 | | | MDA-MB 231 | | |
	24 h	48 h	72 h	24 h	48 h	72 h
AcSh	47.9 ± 5.9	15.9 ± 1.2	7.8 ± 0.9	23.5 ± 2.9	19.7 ± 7.8	21.6 ± 0.8
AcSh/β-CD	40.9 ± 29.4	11.2 ± 1.7	1.2 ± 2.7	35.5 ± 1.8	32.5 ± 10.5	34.5 ± 5.0

[a] Results are from three separate experiment presented as mean ± SD.

1.22 g/mL vs. 7.8 g/mL). However, AcSh/β-CD demonstrated lower cytotoxicity on MDA-MB-231 at each time point of treatment (Table 2). Importantly, free β-CD carrier exhibited no evident cytotoxicity toward both cell lines.

Taken together, these results suggest that AcSh/β-CD effectively inhibits the growth of HCT-116 and MDA-MB-231 cancer cells after short-term treatment. Moreover, examined binary system showed significantly higher cytotoxic effect against HCT-116 cancer cells compared to the cytotoxic effects of free AcSh and β-CD treated cells.

3.5.2. Acetylshikonin/β-cyclodextrin inclusion complex (AcSh/β-CD) more effectively inhibits long term survival of tumor cells

Since the effective short term cytotoxic effects of AcSh/β-CD in HTC-116 and MDA-MB-231 tumor cells were demonstrated by MTT assay, the next goal was to investigate and to com-pare the

long term cytotoxic effects of different concentrations of AcSh/β-CD and free AcSh on cancer cells by clonogenic survival assay.

The results indicated that both free AcSh and inclusion complex significantly decreased survival fractions (SF) of cancer cells investigated in dose dependent manner. Importantly, at the lowest concentration (1 g/mL) the survival fraction of AcSh/β-CD treated cells was 2 fold lower in HCT-116 cells and by up to 20 fold lower in MDA-MB-231 cells in in comparison to survival fractions of free AcSh treated cells (Fig. 7). Therefore, prepared binary system demonstrated superior inhibition of clonogenic survival on both cell lines.

3.5.3. Acetylshikonin/β-cyclodextrin inclusion complex (AcSh/β-CD) have superior effect on cell-cycle arrest in HCT116 and MDA-MB 231 cells

Since the results from the proliferation assays demonstrated strong short-term and superior long-term cytotoxic effect of
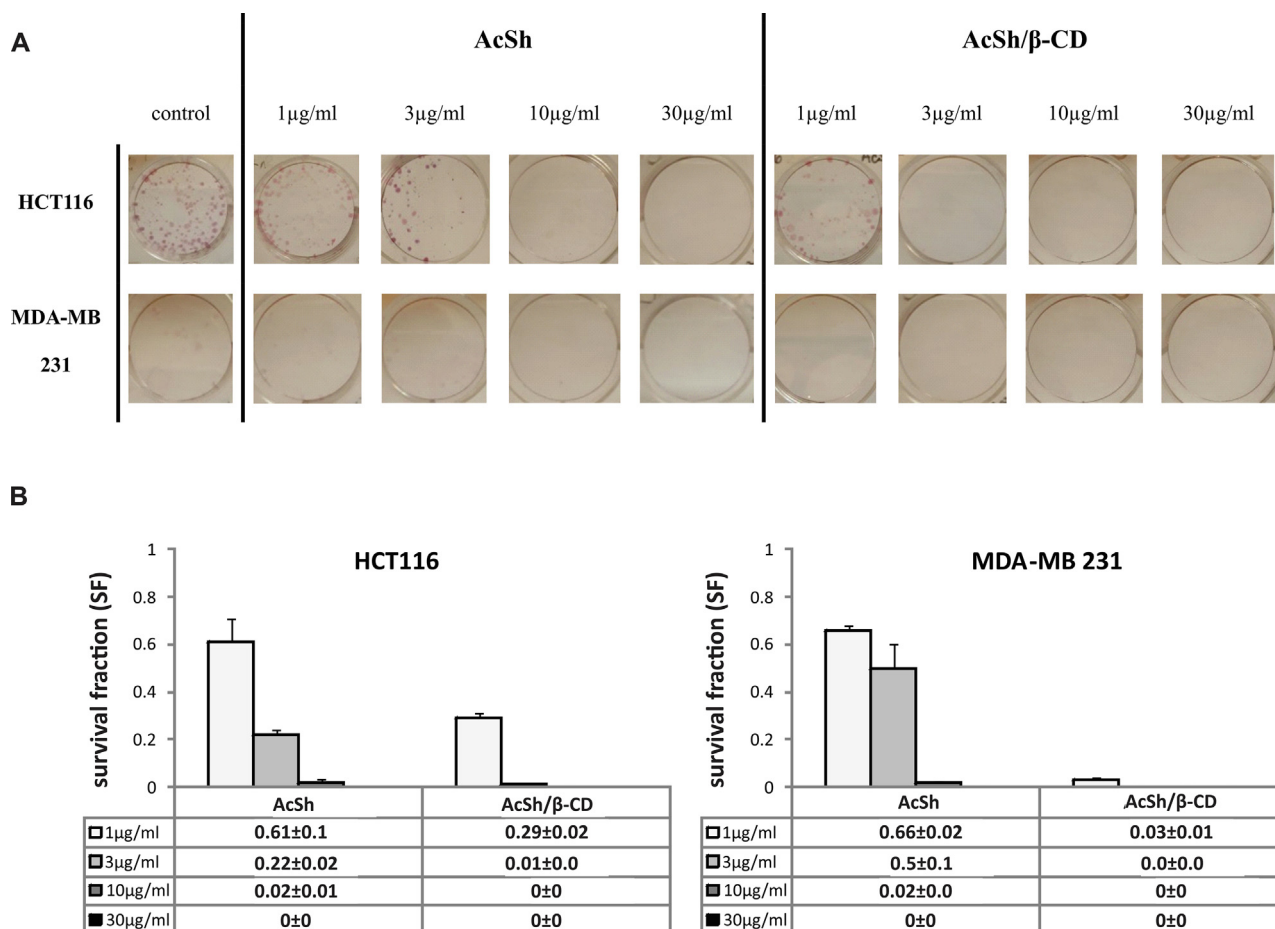

Fig. 7. Clonogenic survival of HCT-116 and MDA-MB-231 cells treated with various concentrations of AcSh and AcSh/β-CD. (A.) Representative images of the clonogenic assay; (B.) Graphs showing survival fractions of AcSh and AcSh/β-CD-treated HCT-116 and MDA-MB-231 cells. Results are from three separate experiment presented as mean ± SD.

AcSh/β-CD in HCT-116 and MDA-MB-231 cells, we next investigated the mechanisms underlying this growth inhibition. Flow cytometric analysis was employed to measure and compare the effect of AcSh and AcSh/β-CD on cell-cycle progression by measuring cellular DNA content in treated cells.

The results indicated that the treatment of HCT-116 and MDA-MB-231 cells with IC_{50} values of AcSh/β-CD for 48 h resulted in a significant arrest of 49.3% of cells in the G2/M and 81.8% of cells in G0/G1 phases of cell cycle, respectively. Comparatively, the HCT-116 cells treated with free AcSh had no significant alterations in cell cycle compared to control, while the cell cycle progress of AcSh treated MDA-MB-231 cells was blocked at the G0/G1 phase (73.5%) (Fig. 8). Therefore, treatment of both cell lines with AcSh/β-CD induces stronger cell cycle arrest compared to free AcSh cells treatment.

3.5.4. Acetylshikonin/β-cyclodextrin (AcSh/β-CD)-induced cytotoxicity depends on the accumulation of intracellular ROS in HCT116 and MDA-MB 231 cells

The overproduction of intracellular ROS (oxidative stress) could be generated not only by abnormal metabolism, but also by various drugs therapy. Oxidative stress has been widely implicated in drug-induced cytotoxicity (Deavall et al., 2012). Therefore, we evaluated the production of ROS in HCT-116 and MDA-MB-231 cells treated with IC_{50} values of AcSh/β-CD for 2 h, 4 h and 6 h and compared it to the ROS production in free AcSh treated and control cells. The results demonstrated that AcSh/β-CD increased the generation of intracellular ROS in both cancer cells with fluorescence intensities increased up to 2 fold in HCT-116 and 1.5 fold in MDA-MB-231 cells, compared to the control. Moreover, AcSh/β-CD treatment of cells increased the ROS production by average of 1.3 fold in HCT-116 and by 1.1 fold in MDA-MB-231 cells in comparison to AcSh treated cells (Fig. 9). Therefore, these results suggest that AcSh/β-CD complex induce increase in accumulation of intracellular ROS more effectively than free AcSh.

3.5.5. AcSh/β-CD inclusion complex induces apoptosis in HCT-116 cells by regulating the expression of Bcl-2, Bax and active caspase-3

Since our results indicated AcSh/β-CD as an effective anti-tumor drug towards HCT-116 and MDA-MB-231 cancer cells, we next evaluated its potential apoptotic effect by flow cytometric analysis of the expression of key regulatory apoptotic proteins, Bcl-2, Bax and active caspase-3 (Papaliagkas et al., 2007), and compared it to the apoptotic effect of AcSh treated cells.

The results indicated that the treatment of HCT-116 cells with IC_{50} values of both AcSh/β-CD and AcSh for 48 h resulted in a significant increase of pro-apoptotic Bax expression, while the expression of anti-apoptotic Bcl-2 was markedly down-regulated consequently leading to the decrease of Bcl-2/Bax protein ratio compared to control cells. Additionally, both AcSh/β-CD and AcSh induced considerable elevation of active caspase-3 in HCT-116 cells compared to control. Moreover, AcSh/β-CD induced 1.2 fold stronger up-regulation of active caspase-3 expression in comparison to the expression of active caspase-3 in AcSh treated cells. However, neither AcSh/β-CD nor AcSh had a significant effect on the expressions of Bcl-2, Bax and active caspase-3 proteins levels in MDA-MB 231 cells (Fig. 10) indicating engagement of some other death pathways.

3.5.6. AcSh/β-CD inclusion complex enhanced the inhibition of autophagy in HCT-116 and MDA-MB-231 cells

Autophagy can be utilized as a survival mechanism in cancer cells and is often upregulated in response to cancer treatment (Degenhardt et al., 2006). Therefore, inhibition of autophagy can be of benefit in cancer treatment (Mulcahy Levy et al., 2017). Autophagy is characterized by formation of acidic vesicular organelles (AVOs) which can be detected and measured by staining with acridine orange. Acridine orange is a vital dye that crosses freely through biological membranes. When accumulated in acidic compartments, it emits bright red fluorescence. Therefore, to detect autophagy and to quantify the accumulation of AVOs, we performed flow cytometric analysis of acridine orange-stained HCT-116 and MDA-MB-231 cells treated with IC_{50} values of both AcSh/β-CD and AcSh for 48 h and compared it to control. As presented in Fig. 11A, although both AcSh and AcSh/β-CD inhibited autophagy, inclusion complex decreased the percentage of red/-green cells in both HCT-116 and MDA-MB-231 cells more efficiently (16.9% and 25.2%, respectively in comparison to AcSh treated cells-28.0% and 42.9%, respectively) (Fig. 11A). Elevated expression of protein p62, an autophagy marker, confirmed autophagy inhibition in both treated cell lines (Fig. 11B).

4. Conclusion

In conclusion, we described the procedure of preparation of acetylshikonin/β-cyclodextrin inclusion complex by using coprecipitation method. The results of phase solubility study revealed on formation of A_L-type binary system. Calculated stability constant Ks of 306.01 M^{-1} indicated that the formation of the inclusion complex increases the aqueous solubility of acetylshikonin. Further, UV/VIS, IR and ^1H NMR spectroscopy confirmed embedding of acetylshikonin in acetylshikonin/β-cyclodextrin inclusion complex. Acetylshikonin encapsulation improved its cytotoxic activity against HCT-116 and MDA-MB-231 tumor cell lines. More
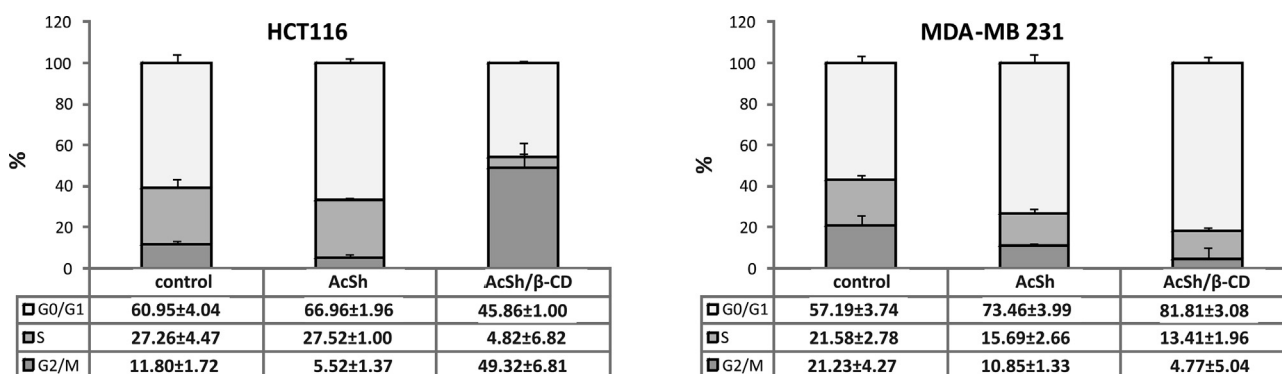

HCT116	control	AcSh	AcSh/β-CD
▢ G0/G1	60.95±4.04	66.96±1.96	45.86±1.00
▢ S	27.26±4.47	27.52±1.00	4.82±6.82
▣ G2/M	11.80±1.72	5.52±1.37	49.32±6.81

MDA-MB 231	control	AcSh	AcSh/β-CD
▢ G0/G1	57.19±3.74	73.46±3.99	81.81±3.08
▢ S	21.58±2.78	15.69±2.66	13.41±1.96
▣ G2/M	21.23±4.27	10.85±1.33	4.77±5.04

Fig. 8. Effects of AcSh and AcSh/β-CD binary system on cell cycle progression in HCT-116 and MDA-MB-231 cells. Graphs are showing the proportion of cells in different phases of cell cycle. Results are from three separate experiment presented as mean ± SD.
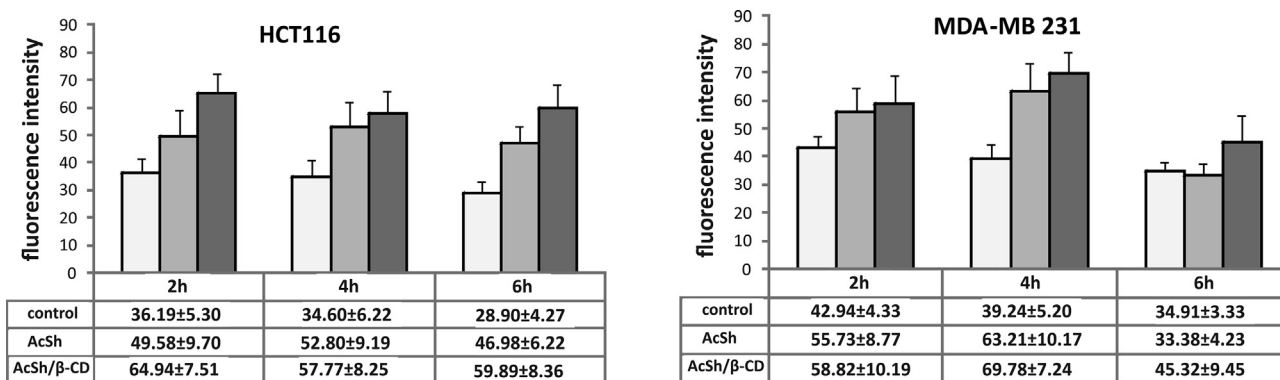
Fig 9. Effect of free AcSh and AcSh/β-CD on intracellular ROS production in HCT-116 and MDA-MB-231 cells. Results are from three separate experiment presented as mean ± SD.
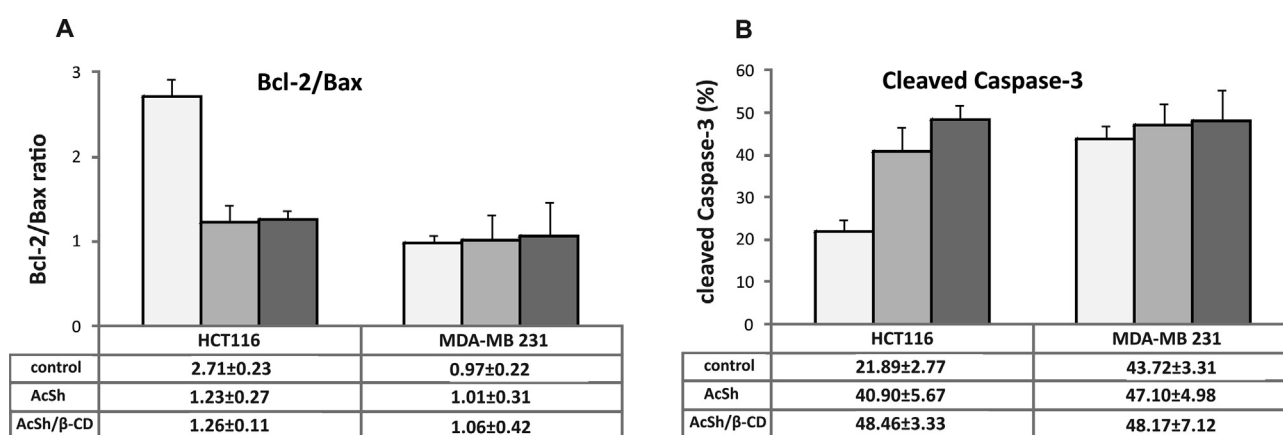

Fig. 10. Expression of apoptosis regulatory proteins in HCT-116 and MDA-MB-231 cells treated with IC_{50} values of free AcSh and AcSh/β-CD for 48 h was analyzed by flow cytometry. (A) Bcl-2/Bax protein levels ratio in treated and control cells; (B) Percentage of treated and untreated cells expressing active caspase-3. Results are from three separate experiment presented as mean ± SD.
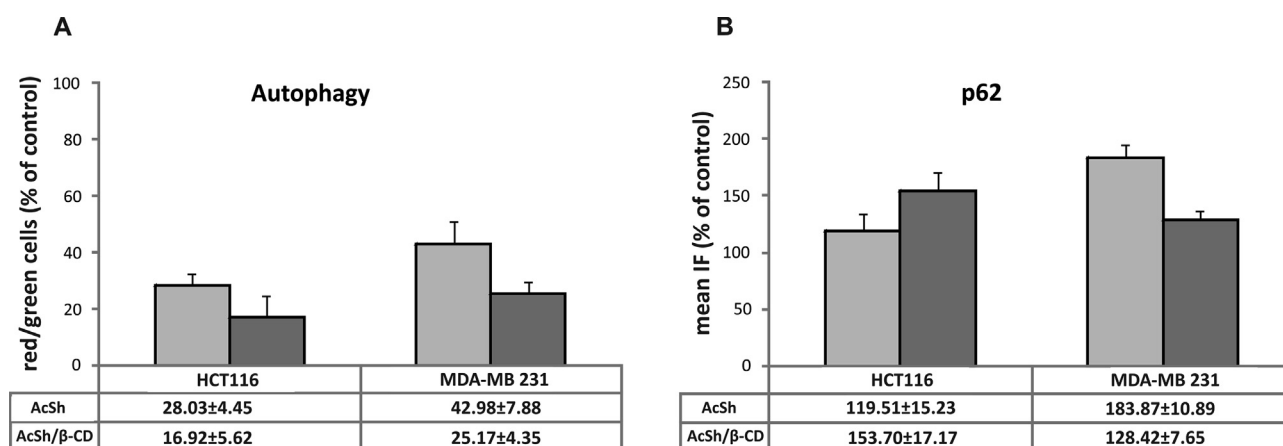

Fig. 11. Effects of AcSh and AcSh/β-CD on autophagy in HCT-116 and MDA-MB-231 cells. (A) Percentage of red/green cells in AcSh and AcSh/β-CD treated HCT-116 and MDA-MB-231 cells in relation to control; (B) expression of p62 protein in AcSh and AcSh/β-CD treated HCT-116 and MDA-MB-231 cells in relation to control. Results are from three separate experiment presented as mean ± SD.

pronounced cell cycle arrest, autophagy inhibition and intracellular ROS generation resulted in superior long-term cytotoxic effect of inclusion complex in relation to free acetylshikonin.

In overall, since encapsulation increases the level of cytotoxic activity toward tested cancer cells, this binary system should be regarded as a useful approach for the design of a novel formulation of acetylshikonin for clinical purposes, with the fact that further studies should be performed in order to examine efficiency of cellular uptake and release of acetylshikonin from the microsphere of β-cyclodextrin.

Declaration of Competing Interest

The authors declare no conflict of interest.

Acknowledgements

References

Amruta, T., Nancy, P., Prashant, K., Niteshkumar, S., 2018. Encapsulation of boswellic acid with - and hydroxypropyl–cyclodextrin: synthesis, characterization, *in vitro* drug release and molecular modelling studies. J. Mol. Struct. 1154, 504–510.

Calabro, M.L., Tommasini, S., Donato, P., Raneri, D., Stancanelli, R., Ficarra, P., et al., 2004. Effects of - and β-cyclodextrin complexation on the physico-chemical properties and antioxidant activity of some 3-hydroxyflavones. J. Pharm. Biomed. Anal. 35, 365–377.

Charan Raja, M.R., Srinivasan, S., Subramaniam, S., Rajendran, N., Sivasubramanian, A., Mahapatra, S.K., 2016. Acetyl shikonin induces IL-12, nitric oxide and ROS to kill intracellular parasite *Leishmania donovani* in infected hosts. RSC Adv. 6, 61777–61783.

Cheirsilp, B., Rakmai, J., 2016. Inclusion complex formation of cyclodextrin with its guest and their applications. Biol. Eng. Med. 2 (1), 1–6.

Chen, C.Y., Chen, F.A., Wu, A.B., Hsu, H.C., Kang, J.J., Cheng, H.W., 1996a. Effect of hydroxypropyl–cyclodextrin on the solubility, photostability and *in-vitro* permeability of alkannin/shikonin enantiomers. Int. J. Pharm. 141 (1–6), 171–178.

Chen, F.A., Cheng, H.W., Wu, A.B., Hsu, H.C., Chen, C.Y., 1996b. Kinetic studies of the photochemical decomposition of alkannin/shikonin enantiomers. Biol. Pharm. Bull. 44, 249–251.

Cheng, H.W., Chen, F.A., Hsu, H.C., Chen, C.Y., 1995. Photochemical decomposition of alkannin/shikonin enantiomers. Int. J. Pharm. 120 (2), 137–144.

Cheng, Y.W., Chang, C.Y., Lin, K.L., Hu, C.M., Lin, C.H., Kang, J.J., 2008. Shikonin derivatives inhibited LPS-induced NOS in RAW 264.7 cells via downregulation of MAPK/NF-B signaling. J. Ethnopharmacol. 120, 264–271.

Davies, K.M., 2004. Important rare pigments, in Davies K.M. (Eds.), Plant pigments and their manipulation. Annual Plant Reviews. Blackwell Publishing Ltd, Oxford, vol. 14, pp. 214-247.

Davis, P.H., 1988. Flora of Turkey and the East Aegean Islands, Vol. 6. Edinburgh University Press, Edinburgh.

Deavall, D.G., Martin, E.A., Horner, J.M., Roberts, R., 2012. Drug-induced oxidative stress and toxicity. J. Toxicol., 1–13

Degenhardt, K., Mathew, R., Beaudoin, B., Bray, K., Anderson, D., Chen, G., et al., 2006. Autophagy promotes tumor cell survival and restricts necrosis, inflammation, and tumorigenesis. Cancer Cell 10 (1), 51–64.

Gong, L., Li, T., Chen, F., Duan, X., Yuan, Y., Zhang, D., Jiang, Y., 2016. An inclusion complex of eugenol into β-cyclodextrin: preparation, and physicochemical and antifungal characterization. Food Chem. 196, 324–330.

Gwon, S.Y., Ahn, J.Y., Chung, C.H., Moon, B., Ha, T.Y., 2012. *Lithospermum erythrorhizon* suppresses high-fat diet-induced obesity, and acetylshikonin, a main compound of *Lithospermum erythrorhizon*, inhibits adipocyte differentiation. J. Agric. Food Chem. 60 (36), 9089–9096.

Han, B., Yang, B., Yang, X., Zhao, Y., Liao, X., Gao, C., et al., 2014. Host-guest inclusion system of norathyriol with β-cyclodextrin and its derivatives: preparation, characterization, and anticancer activity. J. Biosci. Bioeng. 117 (6), 775–779.

Higuchi, T., Connors, K.A., 1965. Phase solubility techniques. Adv. Anal. Chem. Instr. 4, 117–122.

Koike, A., Shibano, M., Mori, H., Kohama, K., Fujimori, K., Amano, F., 2016. Simultaneous addition of shikonin and its derivatives with lipopolysaccharide induces rapid macrophage death. Biol. Pharm. Bull. 39 (6), 969–976.

Kretschmer, N., Rinner, B., Deutsch, A.J., Lohberger, B., Knausz, H., Kunert, O., et al., 2012. Naphthoquinones from *Onosma paniculata* induce cell-cycle arrest and apoptosis in melanoma Cells. J. Nat. Prod. 75 (5), 865–869.

Li, Q., Pu, H., Tang, P., Tang, B., Sun, Q., Li, H., 2018. Propyl gallate/cyclodextrin supramolecular complexes with enhanced solubility and radical scavenging capacity. Food Chem. 245, 1062–1069.

Liu, D.D., Guo, Y.F., Zhang, J.Q., Yang, Z.K., Li, X., Yang, B., Yang, R., 2017. Inclusion of lycorine with natural cyclodextrins (α-, β- and γ-CD): experimental and *in vitro* evaluation. J. Mol. Struct. 1130, 669–676.

Mirzaei, S.A., Reiisi, S., Tabari, P.G., Shekari, A., Aliakbari, F., Azadfallah, E., et al., 2018. Broad blocking of MDR efflux pumps by acetylshikonin and acetoxyisovalerylshikonin to generate hypersensitive phenotype of malignant carcinoma cells. Sci. Rep. 8, 3446.

Mosmann, T., 1983. Rapid colorimetric assay for cellular growth and survival: application to proliferation and cytotoxicity assays. J. Immunol. Methods 65 (1–2), 55–63.

Mulcahy Levy, J.M., Zahedi, S., Griesinger, A.M., Morin, A., Davies, K.D., Aisner, D.L., et al., 2017. Autophagy inhibition overcomes multiple mechanisms of resistance to BRAF inhibition in brain tumors. eLife 6 (e19671), 1–24.

Ozdemira, N., Polab, C.C., Teixeirac, B.N., Hilld, L.E., Bayraka, A., Gomesd, C.L., 2018. Preparation of black pepper oleoresin inclusion complexes based on beta-cyclodextrin for antioxidant and antimicrobial delivery applications using kneading and freeze drying methods: a comparative study. LWT-Food Sci. Technol. 91, 439–445.

Papageorgiou, V.P., Assimopoulou, A.N., Couladouros, E.A., Hepworth, D., Nicolaou, K.C., 1999. The chemistry and biology of alkannin, shikonin, and related naphthazarin natural products. Angew. Chem. Int. Ed. 38, 270–300.

Papaliagkas, V., Anogianaki, A., Anogianakis, G., Ilonidis, G., 2007. The proteins and the mechanisms of apoptosis: a mini-review of the fundamentals. Hippokratia 11 (3), 108–113.

Park, S.H., Phuc, N.M., Lee, J., Wu, Z., Kim, J., Kim, H., et al., 2017. Identification of acetylshikonin as the novel CYP2J2 inhibitor with anti-cancer activity in HepG2 cells. Phytomedicine 24, 134–140.

Rosa, C.G.D., Caroline Borges, D., Zambiazi, R.C., Nunes, M.R., Benvenuttic, E.V., Luza, S.R.D., et al., 2013. Microencapsulation of gallic acid in chitosan, β-cyclodextrin and xanthan. Ind. Crops. Prod. 46, 138–146.

Shanmuga priya, A., Balakrishnan, S.B. Veerakanellore, G.B., Stalin, T., 2018. In-vitro dissolution rate and molecular docking studies of cabergoline drug with β-cyclodextrin. J. Mol. Struct., 1160, pp. 1–8.

Shen, C.C., Syu, W.J., Li, S.Y., Lin, C.H., Lee, G.H., Sun, C.M., 2002. Antimicrobial activities of naphthazarins from *Arnebia euchroma*. J. Nat. Prod. 65 (12), 1857–1862.

Skrzypczak, A., Przystupa, N., Zgadzaj, A., Parzonko, A., Sykłowska-Baranek, K., Paradowska, K., et al., 2015. Antigenotoxic, anti-photogenotoxic and antioxidant activities of natural naphthoquinone shikonin and acetylshikonin and *Arnebia euchroma* callus extracts evaluated by the umu-test and EPR method. Toxicol. in Vitro 30, 364–372.

Su, M.L., He, Y., Li, Q.S., Zhu, B.H., 2016. Efficacy of acetylshikonin in preventing obesity and Hepatic Steatosis in db/db Mice. Molecules 21 (8), 1–14.

Toker, A., Akacay, F., Aksoy, H., Suleyman, H., Ozgen, U., Erdem, H., 2013. The effects of acetyl shikonin isolated from *Onosma armeniacum* on oxidative stress in ethanol-induced ulcer model of rats. Turk. J. Med. Sci. 43, 315–320.

USFDA, 2001. U.S. Food and Drug Administration. Agency response letter GRAS notice 000074. CFSAN/Office of Food Additive Safety. <https://www.fda.gov/downloads/food/ingredientspackaginglabeling/gras/noticeinventory/ucm261320.pdf/> (Accessed date: 5 May 2017).

Vukic, M.D., Vukovic, N.L., Djelic, G.T., Popovic, S.L., Zaric, M.M., Baskic, D.D., et al., 2017. Antibacterial and cytotoxic activities of naphthoquinone pigments from *Onosma visianii* Clem. Excli J. 16, 73–88.

Zhang, L., Man, S., Qiu, H., Liu, Z., Zhang, M., Ma, L., Gao, W., 2016. Curcumin-cyclodextrin complexes enhanced the anti-cancer effects of curcumin. Environ. Toxicol. Pharmacol. 48, 31–38.

Zyzelewicz, D., Oracz, J., Kaczmarska, M., Budryn, G., Grzelczyk, J., 2018. Preparation and characterization of inclusion complex of (+)β-catechin with -cyclodextrin. Food Res. Int. 113, 263–268.